Large Pulse Tube Cooler with a Heat Interceptor

M.B.C. Branco, C. Buti, T. Tirolien, L. Desjonquères , M. Linder

European Space Agency, Noordwijk, The Netherlands

ABSTRACT

Following on the hegemony over many years of the Oxford/Bae Stirling Coolers on Space missions, the Large Pulse Tube Cooler (or LPTC), by Air Liquide, has established itself as Europe's *de facto* workhorse cryocooler, having been chosen for the Meteosat Third Generation, IASI-NG on Metop-SG and being currently considered for plenty other Earth Observation missions as well as Space Science Observatories.

Based on the work carried with heat interceptors on cold fingers by I Charles [1] on the Mini Pulse Tube Cooler, and earlier by D.L. Johnson and R.G Ross Jr. [2] on the Bae Stirling Cooler, an LPTC Engineering Model was tested at the Cryocooler Performance Characterisation Facility at the European Space Research and Technology Center (ESTEC), for its cooling capabilities employing a heat interceptor, at different positions on the cold finger, at temperatures varying from 150 to 200 K.

A significant improvement in performance was measured, compared to the same cryocooler's measured performances without the interceptor, especially at a higher intercept position and for a lower intercept temperature. The heat load at the interceptor was also measured, in order to reflect on the system implications of employing additional cooling at an intermediate temperature, e.g. via a radiator. Considerations on the physical behavior of the pulse tube cooler with the interceptor are also described in this paper, as well as the test setup and the experimental protocol.

INTRODUCTION

The LPTC – Large Pulse Tube Cooler (Figure 1) is a TRL 9 single stage pulse tube cooler optimized for the typical cooled infrared detector range of 50-80K, capable of up to 3 W at 50 K, under certain conditions. Employing a heat interceptor, as in the aforementioned examples, can enable either using the cryocooler for a lower temperature than 50 K with a good cooling power, or improving the efficiency of the cryocooler, for a nominal temperature range of 50-80 K.

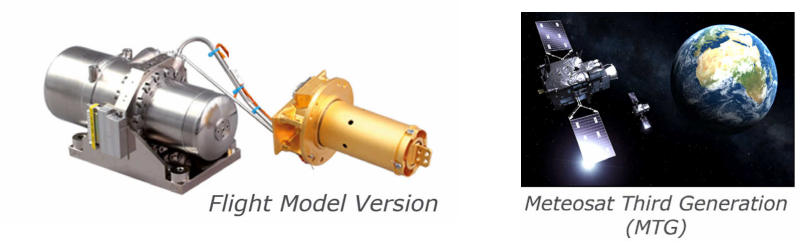

Figure 1. The Large Pulse Tube Cooler and the MTG mission.

Cryocoolers 21, edited by R.G. Ross, Jr., J.R. Raab and S.D. Miller

Heat interceptors work by intercepting parasitic heat loads via the external wall of the cold finger, as well as locally improving some regenerator inefficiencies inside the cold finger itself.

The effectiveness of such a heat interceptor will depend on its location, its temperature, and the heat exchange efficiency from its surface to the cold finger (Figure 2).

As an ideal case an interceptor can be an integral part of the cold finger with a dedicated heat exchanger inside the cold finger, however, simply employing a clamp with a good thermal contact already provides a noticeable increase in performance, according to both papers mentioned as reference.

Our results show a similar trend, where we used Apiezon N to improve on the thermal contact between these surfaces.

Spaceborne applications can benefit from deep space to provide passive cooling via a radiator, as the cold source to the heat interceptor. A nominal range for a single-stage radiator can be considered between 150 to 200 K. It is therefore important to measure the rejected heat load at the intercept, in order to perform the sizing of such a radiator.

TEST SETUP

These tests were performed at the Cryocooler Performance Characterisation Facility (Figure 3), a test facility at ESTEC (Noordwijk – The Netherlands), at the Mechanical Systems Laboratory - https://exchange.esa.int/download/msl/Mechanical_System_Laboratory.pdf.

The Cryocooler Performance Characterisation Facility has been recently devised in order to perform cryocooler characterizations in various conditions, potentially acting as a benchmark for the cryocooler's performance testing. The LPTC Engineering Model 04 (EM04) was tested in a non-intercepted configuration and in an intercepted configuration.

In order to have a proper reference measurement, initial tests were carried under the same conditions but without the heat interceptor applied (Figure 4). These initial tests were performed under controlled heat rejection temperatures at both cold finger warm end and at compressor heat sink, as well as a regulated input power, and the same conditions were then repeated for the actual interceptor test. This allowed to have a better understanding of the performance impact of the heat interceptor.

The heat interceptor clamp design consisted on two halves, fastened together with two small bolts, with a slightly oval shape around the cold finger thin tube, with a gap of 1.0 mm between the straight parts, in the final mounted configuration (Figure 5). This was chosen instead of a snug fit, in order to allow some mounting tolerance and an even clamping, avoiding localized stress concentrations at the cold finger wall.

Concerns regarding the interceptor clamp itself damaging the cold finger walls after cool-down were raised. In this regard, mechanical calculations to evaluate the allowed pre-load at room temperature on the bolts and computing the worst case stresses at the pulse tube thin wall, that were induced after clamping and cool-down, were performed.

The calculations showed comfortable margins, however, validation tests were still performed on 4 coupons of thin-walled piping with slightly different diameters in order to validate the clamping design (Figure 6).

The intercept clamp was fastened with a controlled torque on both bolts and then dipped in liquid nitrogen, there weren't any visible dents or deformations found in any of the tests and the bolts managed to keep the same fastening torque as before the liquid nitrogen immersion.

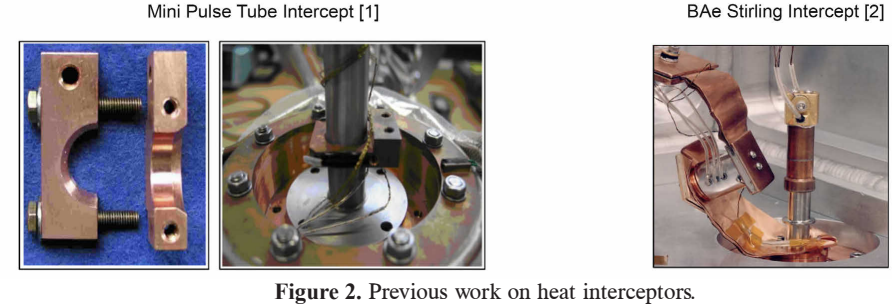

Figure 2. Previous work on heat interceptors.

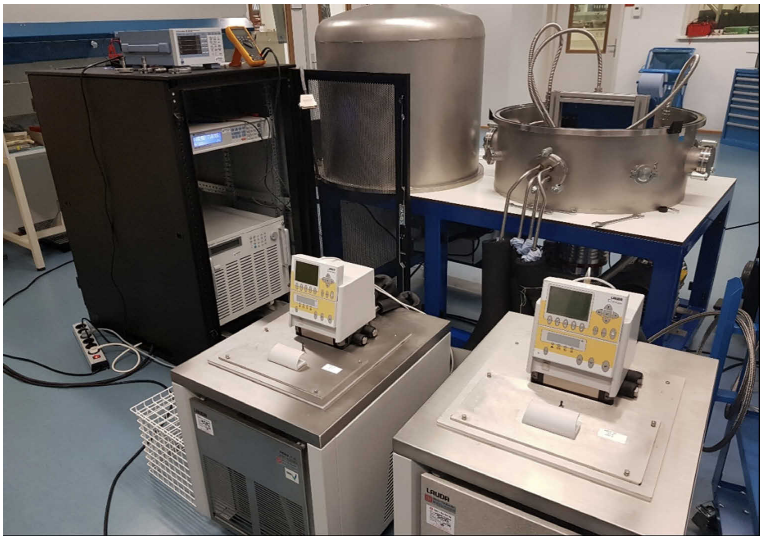

Figure 3. The Cryocooler Performance Characterisation Facility – including separate individual thermostatic chiller control loops for cold finger and compressor, cryogenic thermal monitoring and control units, AC power drive and AC power metering and high vacuum chamber.

The test setup consisted of using a lab cryocooler (Cryomech PT60) as the cold source for the heat interceptor, connected via a long thermal braid and a shorter thermal braid, with cryogenic thermal sensors on both ends, in order to act as a heat flow meter.

Both thermal braids and the intercept, were covered with MLI or SLI in order to decrease the uncertainty on the heat flow measurement and avoiding unnecessary radiative parasitics that could prevent some lower intercept set points (Figure 7). The heat interceptor was equipped with a 5 W heater, for the heat flowmeter calibration, and with a thermal sensor.

The cold finger itself was covered with a high performance MLI (17-layer Helpac1 spacer by RUAG Space GmbH), and this MLI was not changed between reference performance testing and the intercept testing, in order to avoid having some dispersion due to MLI performance and MLI mounting workmanship.

The intercept temperature is regulated via a large 50 W heater placed on the PT60 coldtip, this coarse approach proved to be rather time-consuming as the stabilizing time for a given setpoint

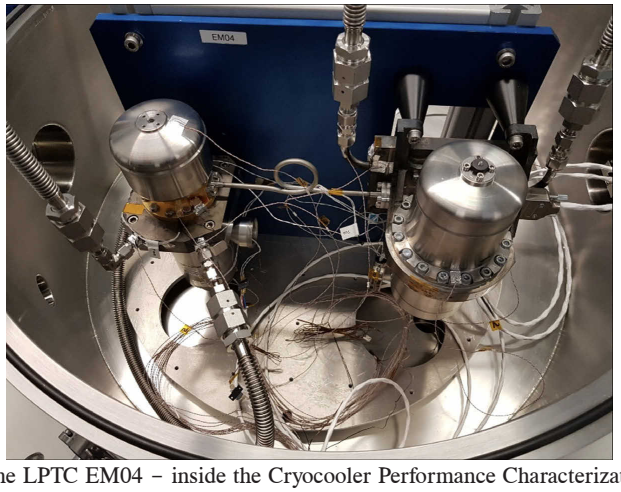

Figure 4. The LPTC EM04 – inside the Cryocooler Performance Characterization Facility in a non-intercepted configuration.

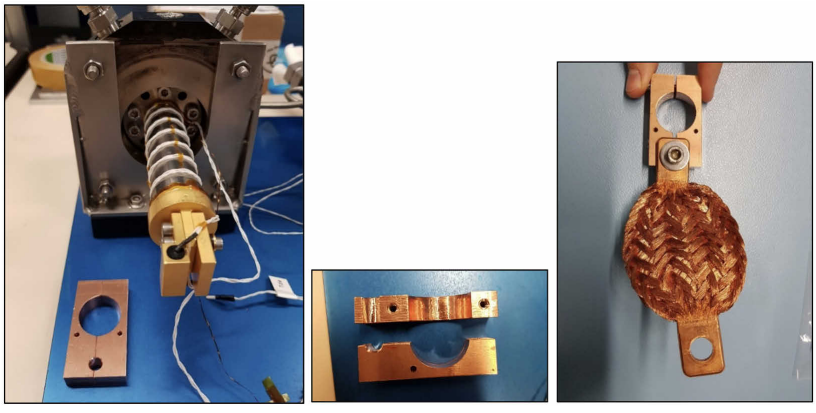

Figure 5. Heat Interceptor clamp, at the left next to the LPTC cold finger, and on the right with the thermal strap attached, which also acted as a heat flow meter.

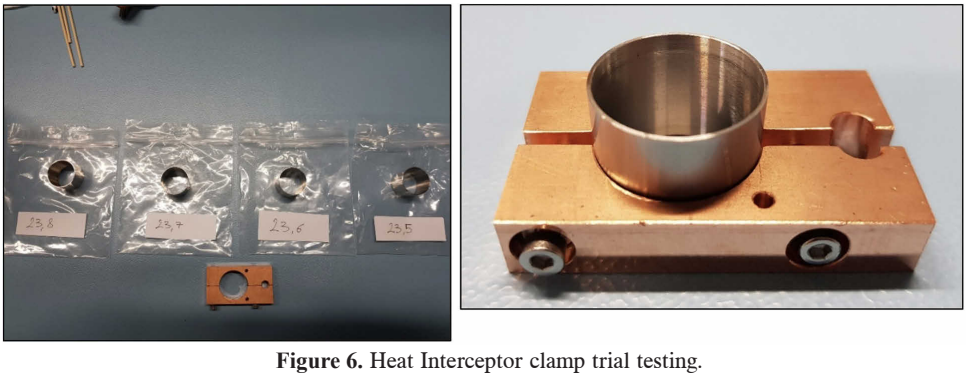

Figure 6. Heat Interceptor clamp trial testing.

was quite long. Using the heater on the intercept as a finer control on the intercept temperature could have been done however it was avoided in order not to deteriorate the intercepted heat flow measurement. A diagram of the test setup is shown in Figure 8.

From a practical stand point 27.5 mm was the highest point the heat interceptor could be mounted without touching any room temperature part. In an ideal case the optimal height might be derived from a SAGE model having already correlated the initial results obtained in this test.

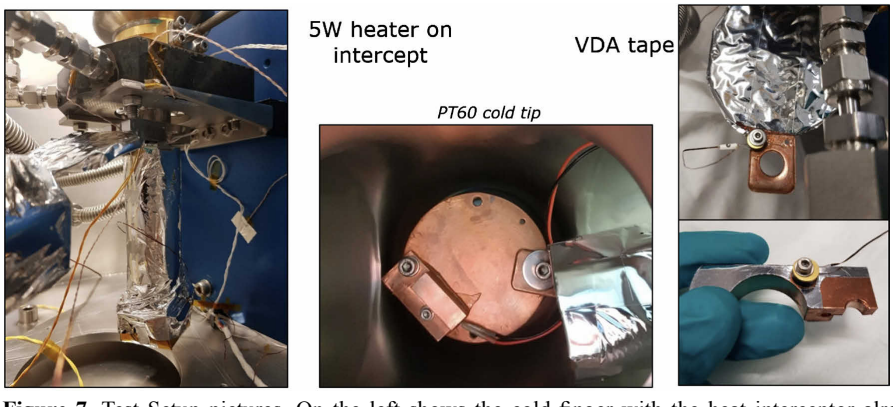

Figure 7. Test Setup pictures. On the left shows the cold finger with the heat interceptor already mounted. In the middle the PT60 cold tip with its heater and the long thermal braid attached, right-top the short thermal braid / heat flow meter, and on the right-bottom the heat interceptor with VDA tape installed.

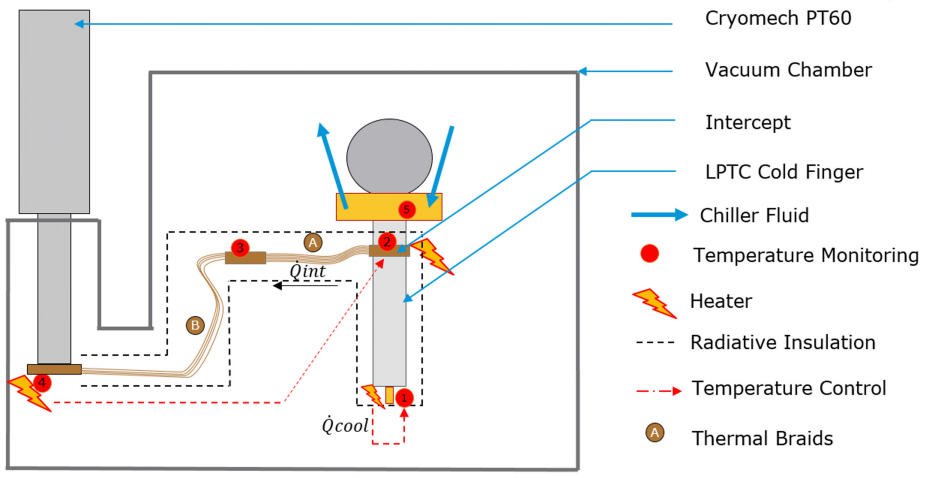

Figure 8. Test Setup diagram.

At the cold tip of the LPTC EM04 a regular heater and cernox sensor were used to measure the cryocooler's cryogenic performance. Room temperature-wise the warm end temperature was controlled using thermocouples and the thermostatic bath chillers with two independent loops for the cold finger warm end and compressor heat sink. The heat interceptor was tested at two different locations on the cold tip, the first tests were performed with a distance from mid height of the intercept to the top most part of the cold finger wall of 32.5 mm. Later these tests were repeated with a raised position of the intercept at 27.5 mm. These heights were not an optimized calculation derived from a SAGE model, but were chosen from similarity from the work performed on the MPTC (smaller class cold finger) and then a second position was taken to study the impact of the interceptor height.

RESULTS

The first tests performed had a regulated warm end temperature at 20 ºC and a compressor input power of 160 W, for an interceptor height of 32.5 mm (Figure 9). Measurement points were taken from no-load point to 2.5 W at the cold tip. The intercept temperature, as it had a very large settling time was quite hard to stabilize at the same setpoint for each measurement point, hence some discrepancy in the same curve, however, in the 170 K intercept curve the same temperature was kept for every measured performance point. As a reference, for all plots, the non-intercepted configuration performance curve is at the right end.

The performance improvement is quite noticeable, especially for the lower intercept temperatures. A minimum no-load temperature of around 23 K is measured, roughly a 7 K decrease from the nominal measured no-load point. As for the cooling performance, one can see a dramatic increase in cooling power, namely for lower temperatures, such as 40 K, where a cooling power

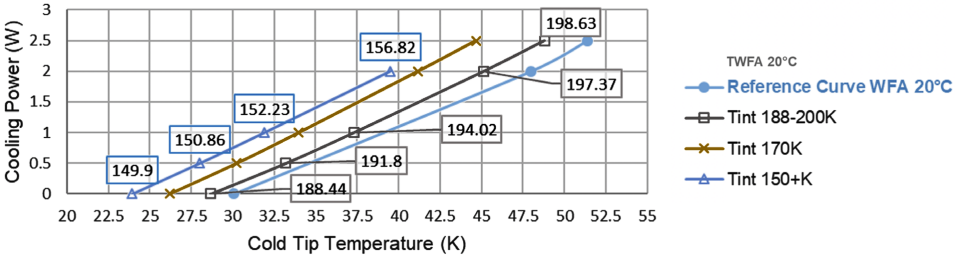

Figure 9. Heat interceptor Performance Results at 32.5 mm and at +20 ºC rejection temperature.

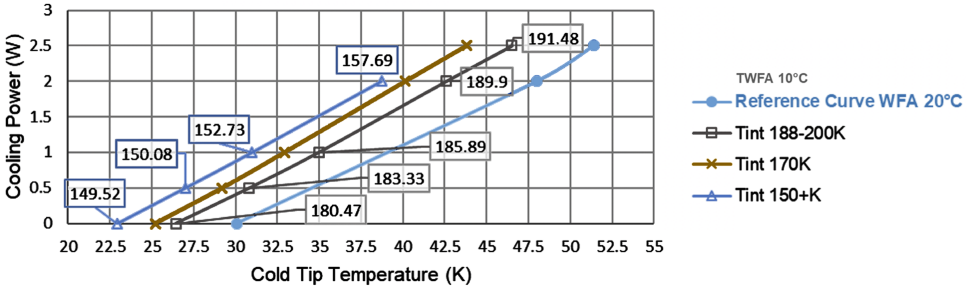

Figure 10. Heat interceptor Performance Results at 32.5 mm and at +10 ºC rejection temperature.

of 2 W is achieved, with the heat interceptor at 150 K vs a measured cooling power of 1 W in the non-intercepted configuration, yielding a cooling performance increase of 100%.

For higher cold tip temperatures this improvement is not so dramatic and will degrade as the intercept temperature is increased.

An interesting test that could have been performed was to raise the intercept temperature until replicating the same cooling performance curve as the non-intercepted configuration, which would indicate towards the expected average temperature at this point in the cold finger. The measured intercepted heat load should also point to a negligible value in order to confirm this.

For the impact of warm end rejection temperature the same tests were performed with the cold finger warm end rejection temperature at 10 ºC (Figure 10), and a slight improvement is measured achieving the same cooling powers at around 1.0 K lower in cold tip temperature. This effect, although beneficial, remains marginal with respect to the impact of the intercept. This can also lead to an optimization of the warm end temperature control system, as its setpoint is not as critical for the cryogenic performance as compared to a non-intercepted configuration.

The higher intercept position shows a similar performance improvement at higher intercept temperatures (Figure 11). By raising the intercept position of 5.0 mm, the same cooling performance is reached at a higher intercept temperature of 20 K. This is particularly interesting for a passive cooling via radiation to deep space application, where a higher temperature leads to a more optimum sizing. An additional and important information for the cold source sizing is the intercepted heat load.

The intercepted heat loads were indirectly measured thanks to the thermal gradient measured on the short thermal braid, that was previously calibrated as a heat flowmeter in order to derive a W/K slope and remove the constant offset generated by parasitic heat loads notwithstanding the cold finger itself.

In Figure 12 one can see a comparison of the measured heat loads for two matching performance curves, for both intercepted heights of 32.5 mm and 27.5 mm, at the respective intercepted temperatures of 170 K and at 190 K.

The intercepted heat load is higher for the higher position of the intercept, as expected, at about 1 W more, for an intercepted temperature at 20 K higher. Sizing a radiator to provide this cooling clearly favors a higher intercept position.

The intercepted heat load tends to scale linearly with the cold tip temperature and to be higher in the highest position of the intercept.

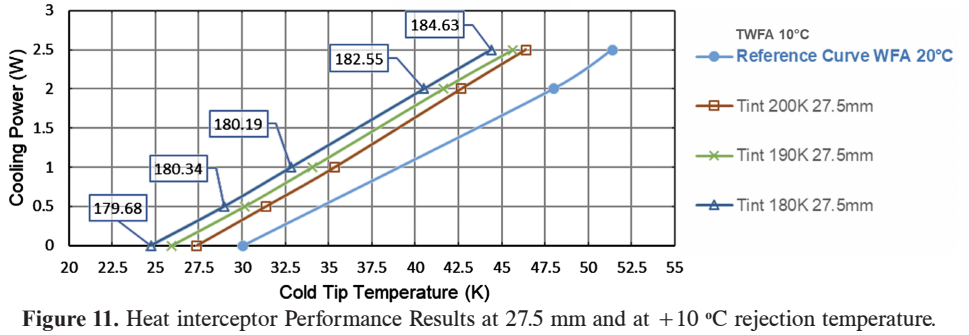

Figure 11. Heat interceptor Performance Results at 27.5 mm and at +10 ºC rejection temperature.

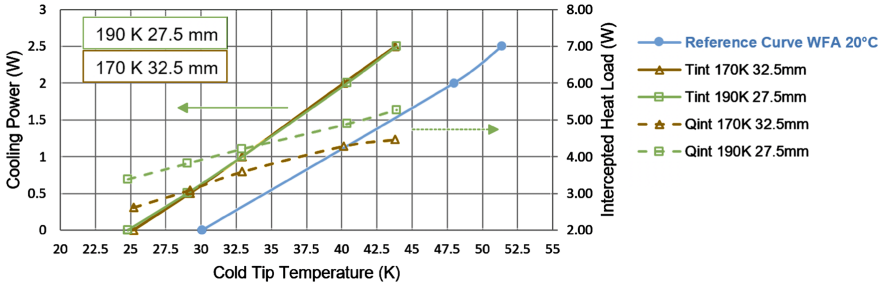

Figure 12. Measured heat loads for two matching performance curves, for both intercepted heights of 32.5 mm and 27.5 mm, at the respective intercepted temperatures of 170 K and at 190 K.

The measured values fall in a range roughly 3 to 7 W at temperatures from 150 to 200 K, which is a pretty reasonable sizing case for a single-stage cryogenic radiator with a stable pointing to deep space and shielded from solar and earth heat fluxes.

Regarding the nature of these intercepted heat loads, one can argue that these do not fully correspond to either just blocking parasitic heat loads, which would yield a much lower heat load, or to acting as a "PV work rejection" stage, which would result in a much higher heat load. It seems the intercept effect is two-fold, acting on the hand as a parasitics cut-off point, as well as on the other hand locally improving the regenerator inefficiencies.

Correlating these measurements with a SAGE model could yield a better understanding of the main contributors to the interceptor heat load, in order to find an optimal position.

COLD REDUNDANCY – IDLE COOLER PARASITICS

Typical cooled infrared detection systems employ a cold redundancy scheme, with one operating cooler and a second redundant one, to avoid single-point failures and improve the overall reliability. An important consideration when using a single-stage cryocooler at lower temperatures than 50 K is the added parasitic heat loads brought by an idle redundant cryocooler, and its contribution to the total cooling budget increases significantly in a non-intercepted configuration as the cold tip temperature is lowered.

Employing an intercept decreases significantly the budget contribution of the idle cooler parasitics. This works in two ways, by intercepting the cold finger at an intermediate temperature and decreasing the parasitics, as well as improving the cooling performance for that given temperature, which in the end yields a much lower contribution to the overall budget.

As can be derived from Figure 13, when using such a cold finger for temperatures lower than 50 K in a cold redundancy scheme, the idle cooler's parasitics become forbiddingly high (considering a warm end rejection temperature of +20 ºC), which prevents using a single-stage cooler for such lower temperature applications, even though it can still deliver a reasonable amount of cooling power, the parasitics from the redundant cooler become just too dominating.

Employing an interceptor in this case can prove to be an enabler, as it drastically reduces the impact of the redundant cooler parasitics in two ways, first, by cutting off part of the parasitic heat load, and secondly, by improving the cryocooler's cooling performance.

It should also be noted that the total intercepted heat load in this configuration will be higher than the presented measured values due to the added redundant cooler parasitics.

It should be noted that parasitic heat load measurements were not performed in this set of tests due to lack of an additional cold source at 30 K, so the presented pie charts (Figure 14) are a result of scaling the known parasitic heat loads for the LPTC EM04 in a non-intercepted configuration, to the intercept configuration (new length ratio and temperature difference).

Parasitic heat load measurements in a steady state will be quite useful to confirm this estimate and the advantages of employing an intercept in a cold redundancy scheme.

It should be noted that, thanks to some design improvements, the LPTC flight models have a slightly lower parasitic heat load and higher cooling power than the LPTC EM04 used for these tests. This makes the impact of the interceptor less dramatic for the flight case as in the EM04, although arguably still highly beneficial.

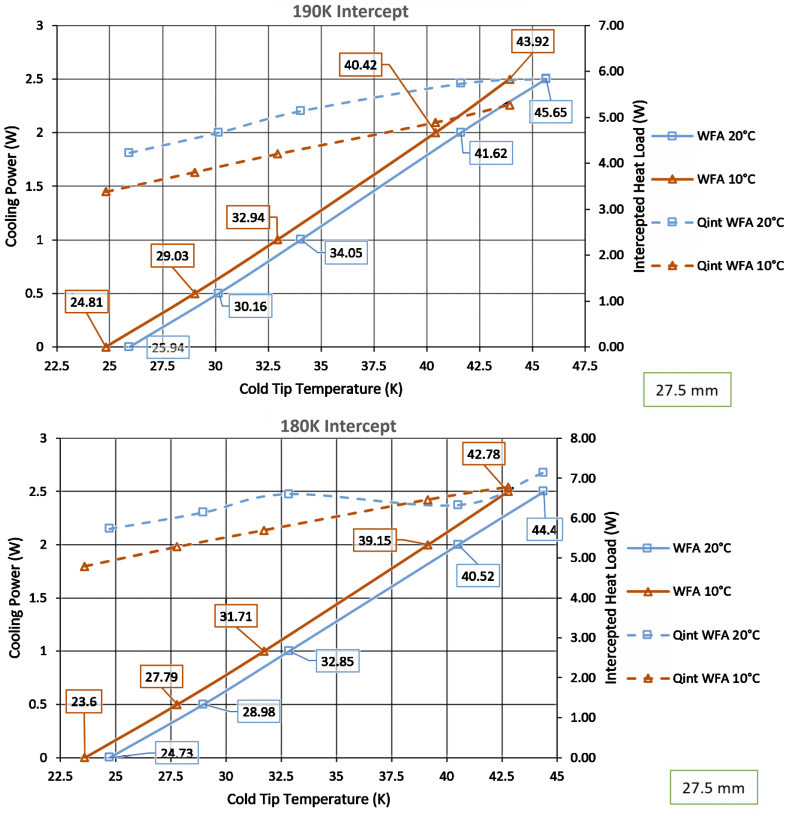

Figure 13. Measured Intercepted Heat Loads (secondary axis) for different set points.

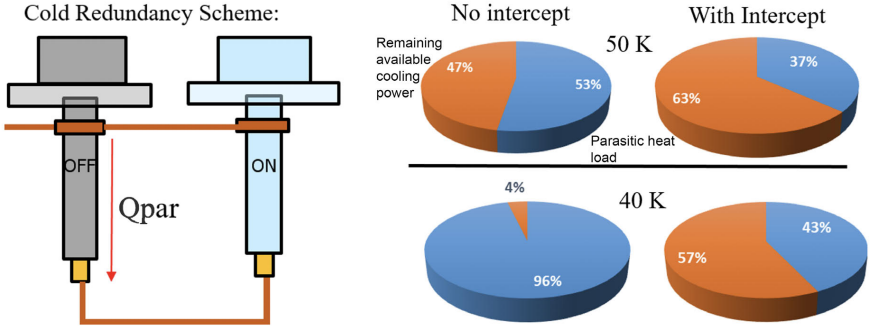

Figure 14. Comparison between parasitic heat load contribution for a cold redundancy scheme, in a non-intercepted configuration vs an intercepted configuration at 50 K and at 40 K.

CONCLUSIONS

Testing with an intercept has shown that a realistic performance improvement of up to 50% in cooling power can be achieved, especially when considering temperatures below 50 K, e.g. 2 W at 40 K, intercept at 180 K, 27.5 mm and 6.5 W intercepted heat load.

Warm rejection temperature is marginally beneficial with respect to a non-intercepted configuration, which could relax the warm end temperature control system.

The higher intercept positions at 27.5 mm has proven to be beneficial for radiator sizing, in order to provide passive cooling in the 170 – 200 K range, as an example, a 0.5 m² radiator facing deep space, shielded from solar and earth heat fluxes, with appropriate design margins could

withstand most cases measured here (assuming many degradation aspects such as heat transport gradients, degradation of emissivity, trimming, radiator efficiency due to temperature uniformity).

In a cold redundancy scenario, an intercept configuration decreases significantly the idle cooler's parasitic heat loads contribution to the total cooling budget. As measured via the heat flow meter, the intercepted heat points to the conclusion that the heat interceptor is not only intercepting parasitic heat loads but actually contributing to the heat regeneration efficiency inside the cold finger. This leads to the conclusion that the heat interceptor will still provide a significant advantage for an optimized cold finger.

Apart from the thermodynamics, concerns rise regarding the structural implications of attaching a bulky item such as this intercept on the cold finger wall and if the cold finger can withstand combined mechanical launch loads with internal pressure plus the clamping and mass attached.

ACKNOWLEDGMENTS

We would like to acknowledge the support from Air Liquide Advanced Technologies, CEA SBT, the Science Directorate at ESA and our great colleagues from the Mechanical Systems Laboratory, Stephane Roure, George Varewijk and Nicolas Rieux, who helped us whenever needed.

REFERENCES

1. I. Charles et al., "A New Mini Pulse Tube with a Heat Interceptor,",*CEC,* Vol. 53*,* (2008).

2. D. L. Johnson and R. G. Ross, Jr., "Cryocooler Coldfinger Heat Interceptor," *Cryocoolers 8,* Plenum Press, New York (1995), pp. 709-717.